Original Clinical Article

3D reconstruction of MR-visible Fe_3O_4-mesh implants: pelvic mesh measurement techniques and preliminary findings[1]

Kerstin A. Brocker 0000-0002-3543-4381 0000-0002-3543-4381, MD, MSc[1], Theresa Mokry, MD[2], Céline D. Alt 0000-0001-5273-0353 0000-0001-5273-0353, MD[3],
Hans-Ulrich Kauczor, MD[2], Florian Lenz[4], Christof Sohn, MD[1],
John O. DeLancey, MD[5], Luyun Chen 0000-0001-6861-180X 0000-0001-6861-180X, PhD[6]

[1]University of Heidelberg, Medical School, Department of Obstetrics and Gynecology, Heidelberg, Germany

[2]University Hospital Heidelberg, Department of Diagnostic and Interventional Radiology, Heidelberg, Germany

[3]University Duesseldorf, Medical Faculty, Department of Diagnostic and Interventional Radiology, Duesseldorf, Germany

[4]Department of Obstetrics and Gynecology, St. Marienkrankenhaus Ludwigshafen, Academic Teaching Hospital of the Faculty of Medicine Mannheim of the University Medical School Heidelberg, Ludwigshafen am Rhein; Germany

[5]University of Michigan, Obstetrics and Gynecology Department, Pelvic Floor Research Group. Ann Arbor, MI, USA

[6]University of Michigan, Pelvic Floor Research Group, Biomedical Engineering Department, Ann Arbor, MI, USA

Short title: 3D reconstruction and pelvic measurements of Fe_3O_4-mesh implants

Word count: 2,740

Acknowledgements: Dr. DeLancey's and Dr. Chen's research efforts were partially supported by the Eunice Kennedy Shriver National Institute of Child Health and Human Development (NICHD) grants P50 HD044406 and R21 HD079908, respectively. The NICHD played no role in the conduct of the research or in the decision to publish. The authors would like to thank Dr. Bing Xie for 3D model smoothing. This study was honored with the *Best in Category Award "Imaging"* at the International Continence Society Annual

[1] This is the author manuscript accepted for publication and has undergone full peer review but has not been through the copyediting, typesetting, pagination and proofreading process, which may lead to differences between this version and the Version of Record. Please cite this article as doi:10.1002/nau.23868

Meeting in Florence, Italy, in September, 2017 and the *Eugen-Rehfisch Award* at the Forum Urodynamicum annual meeting in Wiesbaden, Germany in March, 2017.

Ethical Board approval number S-473/2007, amendment September 28th, 2016

Corresponding Author:
Luyun Chen, PhD
University of Michigan
Department of Obstetrics and Gynecology, Pelvic Floor Research Group
Department of Biomedical Engineering
2350 Hayward St.
Ann Arbor, MI, 48103, USA
Phone: 001-734-763-0366
luyunc@umich.edu

Kerstin A. Brocker, MD, MSc[1], Theresa Mokry, MD[2], Céline D. Alt, MD[3],
Hans-Ulrich Kauczor, MD[2], Florian Lenz[4], Christof Sohn, MD[1],
John O. DeLancey, MD[5], Luyun Chen, PhD[6]

[1]University of Heidelberg, Medical School, Department of Obstetrics and Gynecology, Heidelberg, Germany

[2]University Hospital Heidelberg, Department of Diagnostic and Interventional Radiology, Heidelberg, Germany

[3]University Duesseldorf, Medical Faculty, Department of Diagnostic and Interventional Radiology, Duesseldorf, Germany

[4]Department of Obstetrics and Gynecology, St. Marienkrankenhaus Ludwigshafen, Academic Teaching Hospital of the Faculty of Medicine Mannheim of the University Medical School Heidelberg, Ludwigshafen am Rhein; Germany

[5]University of Michigan, Obstetrics and Gynecology Department, Pelvic Floor Research Group. Ann Arbor, MI, USA

[6]University of Michigan, Pelvic Floor Research Group, Biomedical Engineering Department, Ann Arbor, MI, USA

Short title: 3D reconstruction and pelvic measurements of Fe_3O_4-mesh implants

Word count: 2,740

Acknowledgements: Dr. DeLancey's and Dr. Chen's research efforts were partially supported by the Eunice Kennedy Shriver National Institute of Child Health and Human Development (NICHD) grants P50 HD044406 and R21 HD079908, respectively. The NICHD played no role in the conduct of the research or in the decision to publish. The authors would like to thank Dr. Bing Xie for 3D model smoothing. This study was honored with the *Best in Category Award "Imaging"* at the International Continence Society Annual Meeting in Florence, Italy, in September, 2017 and the *Eugen-Rehfisch Award* at the Forum Urodynamicum annual meeting in Wiesbaden, Germany in March, 2017.

Ethical Board approval number S-473/2007, amendment September 28th, 2016

Corresponding Author:
Luyun Chen, PhD
University of Michigan
Department of Obstetrics and Gynecology, Pelvic Floor Research Group
Department of Biomedical Engineering
2350 Hayward St.
Ann Arbor, MI, 48103, USA
Phone: 001-734-763-0366
luyunc@umich.edu

Abstract

Aims:

To develop MR-based measurement technique to evaluate the postoperative dimension and location of implanted magnetic resonance (MR)-visible meshes.

Methods:

This technique development study reports findings of six patients (A-F) with cystoceles treated with anterior vaginal MR-visible Fe_3O_4-polypropylene implants. Implanted meshes were reconstructed from three months and/or one year postsurgical MR-images using 3D Slicer®. Measurements including mesh length, distance to the ischial spines, pudendal and obturator neurovascular bundles and urethra were obtained using software Rhino® and a custom Matlab® program. The range of implanted mesh length and their placements were reported and compared with mesh design and implantation recommendations. With the anterior/posterior-mesh-segment-ratio mesh shrinkage localization was evaluated.

Results:

Examinations were possible for patients A-D three months and for A, C, E and F one year postsurgical. The mesh was at least 40% shorter in all patients three months and/or one year postoperatively. A, B showed shrinkage in the anterior segment, D, E in the posterior segment (Patients C, F not applicable due to intraoperative mesh trimming). Patient E presented pain in the area of mesh shrinkage. In Patient C posterior mesh fixation was placed in the iliococcygeal muscle rather than sacrospinous ligaments. Arm

placement less than 20 mm from the pudendal neurovascular bundles was seen in all cases. The portion of the urethra having mesh underneath it ranged from 19% to 55%.

Conclusions:

MRI-based measurement techniques have been developed to quantify implanted mesh location and dimension. Mesh placement variations possibly correlating with postoperative complications can be illustrated.

Keywords:

Pelvic organ prolapse, MRI-visible mesh, MRI, 3D reconstruction, measurement

Introduction

Pelvic organ prolapse (POP) occurs when the viscera move downward and protrude through the urogenital opening. This causes distress, abnormal organ function, impaired quality-of-life - affecting millions of women worldwide.[1-3] Vaginal or transabdominal operations with or without synthetic meshes are used to restore pelvic floor support.[1] Yet, vaginal trocar-guided meshes are a controversial topic due to risks of postoperative complications such as mesh contraction/shrinkage, pudendal or obturator neurovascular lesions due to arm placement variations, dyspareunia, or de-novo voiding dysfunction.[4-6]

Imaging studies providing objective evaluations of these issues could help us understand how and why complications arise.[1,4,7] Ultrasound as a standard imaging tool in urogynecology[8] has demonstrated its ability to visualize the mesh material and describe its relation to adjacent pelvic organs.[9,10] However, it is limited when attempting to visualize mesh deep in the body, including the anchoring points and their relationship to neurovascular structures.[11] The pudendal and obturator neurovascular bundles, for example, are at risk of being injured intraoperatively due to their proximity to the recommended mesh arm anchoring points.[12,13]

Newly developed magnetic resonance (MR)-visible Fe3O4-polypropylene partially absorbable meshes in combination with pelvic MR-imaging (MRI) allow visual observation of the full mesh course through the female pelvis, yet objective measurement schemes are scarce.11 In this study, we aim to develop measurement techniques to 1) quantify the dimensions of the implanted mesh to evaluate changes in size compared to its pre-implant dimension ("shrinkage"); 2) measure the distance from implanted mesh to important pelvic structures and compare them with mesh implantation recommendations; and 3) correlate the measurement information with patients' clinical results.

Material and Methods

Study patients

This is a technique development study based on six patients from an ongoing prospective multi-center clinical trial (Ethical Board approval number (Blinded fro review) evaluating women with anterior vaginal mesh repair using an MR-visible Fe3O4-polypropylene implant. MRI and clinical examinations were performed before surgery, three months post surgery, and one year post surgery. All six patients returned for the three-month follow-up and two patients (Patients B & D) opted out for the one-year visit. The inclusion criteria included symptomatic ≥POP-Q stage 2 cystocele with apical prolapse, vaginal mesh surgery with an MR-visible implant, no contraindication for surgery or MRI, and age ≥18 years.

Mesh information and implantation

Two types of partially absorbable (PA) anterior vaginal meshes (Seratom® E PA MR or Seratom® P PA MR by Serag Wiessner GmbH & Co. KG, Naila, Germany) were used. These two meshes only differ in size and shape (e.g., 103 mm vertical mesh length and diamond-shaped body of the Seratom E PA vs. 90 mm vertical mesh length and rectangular-shaped body in the Seratom P PA; Supplemental Figure 1). Both meshes have six arms and MR-visible Fe_3O_4 threads integrated into the weave, alternating with absorbable fibers expected to be absorbed approximately 120 days postsurgically.[11,12,14,15] Mesh implantations were performed according to the manufactuerer's recommendations by expert surgeons (>1000 anterior vaginal meshes implanted). The posterior arms were to be placed through the sacrospinous ligaments approximately 2 cm away from the ischial spine, and the middle and anterior arms were to be placed via the obturator muscle-membrane-complex using a multi-incision trocar-guided technique with reusable introducers/needles.[11-14]

Magnetic Resonance Imaging

All MRIs were acquired in supine position using a 1.5 Tesla scanner (Siemens Symphony, Siemens Medical Solutions, Erlangen, Germany).[11] High-resolution T2-weighted (T2w) turbo spin echo sequence on axial, coronal, and sagittal planes were acquired according to the body axis to visualize the pelvic anatomy (TR 3460-4219 ms, TE 77–88 ms, matrix 512*282, slice thickness 5-6 mm), whereas T1-weighted (T1w) FLASH 2D (TR 128-132 ms, TE 4.7 ms, matrix 256*154, slice thickness 6 mm) and FLASH 3D sequences (TR 15 ms, TE 6 ms, matrix 512*384, slice thickness 1 mm) were performed to visualize the implanted meshes.[11] This study focused on the analysis of the three-month and one-year postoperative MRIs. The three-month follow-up MRIs for patients E and F were excluded from analysis due to poor image quality caused by MR scanner maintenance issues.

Mesh 3D reconstruction and measurements

In all eligible MRIs at three months and one year post surgery, the meshes were visible and 3D mesh models could be reconstructed, making a direct comparison of the implants within the same patient possible (Fig. 1). All MRIs were first imported into 3D Slicer® (version 4.5.1) for visualization and 3D model reconstruction. Then, two additional post-processing programs (the modeling software Rhino® and a custom Matlab® program) were used to perform the quantitative analysis. We used bony landmark-based method to align all MRIs instead of automatic rigid/deformable registration methods to limit the influence of soft tissue variation of the pelvic organs, such as abdominal wall motion, movement of intestines, variation of bladder filling and intestine contents variation. In 3D Slicer®, we first manually identify the bony landmarks including the most inferior part of the pubic symphysis, ischial spines, and the sacrococcygeal junction on

all MRI sequences.[11,16] Then a semi-automatic landmark-based rigid registration method in 3D Slicer® was used to align all MRI sequences at both the three-month and one-year postoperative exams in the same 3D space with standardized bony pelvis orientation.[11,16] . Similarly, MRIs from the three-month and one-year postoperative exams were aligned. Using the point cloud technique, we reconstructed the full mesh course by identifying the mesh on T1w MRIs as hypointense spots compared to surrounding tissue.[11] Figure 1 demonstrates the comparison of reconstructed mesh models obtained from MRI scans three months and one year post surgery in the same patient. Additionally, anatomical structures including pudendal and obturator neurovascular bundles, bladder and urethra with UVJ were reconstructed based on T2w MRIs.[11,17-19] Two observers with extensive experience on pelvic floor MRI anatomy first independently identified the point clouds and outlined the structures. Then the point clouds and models were reviewed, the consensus was reached and reported as final data.

To measure the implanted mesh dimension, mesh point clouds were imported into the modeling software Rhino® (R13, Robert McNeel & Associates, Seattle, USA). Currently, it is not possible to depict the individual mesh threads; therefore, a smooth surface fitted on the point clouds was reconstructed for the mesh body and arms to represent the “effective mesh surface” - the overall shape and dimension - without considering the thread pattern and interaction between mesh threads (Fig. 2). To evaluate the potential mesh shrinkage/folding, the effective length in the middle of the implanted mesh was measured and compared to the mesh length of the product before implantation. We noted the anterior segment (the distance between the anterior and middle arms) and the posterior

segment (the distance between the middle and posterior arms) to compare to the designed parameters (Fig. 2) allowing us to locate where shortening occurred.

All available postsurgical examinations three months and/or one year postoperatively were quantified. The dimension and location of the implanted mesh were measured and compared to original dimension and implantation recommendation. The range and number of patients within the recommendations were reported based on the first available post-operative MR measurements. Standardized t-test was used to compare the original and implanted mesh dimension.

A Matlab® (version 2016) program was developed to evaluate the postoperative mesh placements by calculating the minimum distance between the mesh point cloud and important anatomical structures, such as pudendal and obturator neurovascular bundles (Fig. 3). To evaluate whether the posterior mesh arm implantation achieved the product placement recommendations, we identified the posterior arm penetration points as the location where the posterior arm changes direction (Fig. 3, panel c). Next, the distances from the posterior arm penetration points to the ischial spines were reported.[12] We also evaluated whether the posterior arm penetration point was within the sacrospinous ligament as recommended.[12,13] To evaluate the mesh location relative to the ureterovesical junction (UVJ), we measured the length of the mesh beneath the UVJ and reported it as the percentage of the urethra with mesh underneath it (Fig. 4).

Results

Clinical Evaluation

We evaluated six women (aged 66-76 years) after anterior pelvic floor reconstruction with an MR-visible mesh (for surgery performed and concomitant procedures, see Supplemental Table 1). In two cases (Patients C and F, Supplemental Table 1), the surgeon decided intraoperatively to trim the anterior mesh part and arms, reducing the mesh length by approximately 2 cm, because it was too large to fit the woman's anatomy. No women showed short term intra- or postoperative complications.

All patients attended the three-month postoperative follow-up, which showed no clinical impression of recurrent or de-novo POP (Supplemental Table 1). Patients A, C, E, and F returned for the one-year follow-up. One woman complained about symptoms (dyspareunia, feeling of a bulge in the vagina, and defecational problems) deriving from a recurrent cystocele grade III° and recurrent recto-enterocele grade II°, detected on follow-up clinical examination. Also, the posterior arms could be felt as a tight band that caused pain during Patient E's examination (Supplemental Table 1).

MRI measurement results

For first available post-operative MRI evaluation, the median implanted mesh length was 55 mm (range, 45-58 mm) for Seratom E PA mesh (patients A, C*Trim, E), and 53 mm (range 38 – 54 mm) for Seratom P PA mesh (patient B, D, F*Trim). They are significantly (at least 40%, $p < 0.001$) shorter than the original mesh length. Please keep in mind, for Patient C*Trim and F*Trim, we consider the original mesh length as trimmed mesh length that is 20 mm shorter than designed length (Table 1, Supplement Table 1). Variations in middle arm location in the implanted meshes were observed in Patient E, demonstrating corresponding clinical findings (Fig. 2， Supplemental Table 1). The anterior and posterior segments have a similar designed length (Supplemental Figure 1), resulting in an

anterior/posterior segment ratio close to 1. However, the implanted meshes of patients A and B show a shorter anterior than posterior segment, resulting in an anterior/posterior segment ratio much smaller than 1 (Table 1, Fig. 2, panels a-c). In contrast, in patient E, the posterior segment (9 mm) was much shorter than the anterior segment (49 mm) (Table 1, Fig. 2, panels d-f); this corresponded to the area of pain during palpation in the clinical exam (Supplemental Table 1).

The distances of the mesh from the obturator, pudendal neurovascular bundles, and ischial spines are listed in Table 1 and described in Figure 3. The distance of the mesh arms to obturator neurovascular bundles ranged from 11 mm to 33 mm. In five out of six patients these measurements were larger than recommended - providing sufficient safety margins. Similarly, the distance of mesh arms to the ischial spines ranged from 9 mm to 34 mm with four out of six patients presenting measurements larger than the recommendation. However, posterior mesh arms are significantly closer to pudendal neurovascular bundles than recommended in all six patients, with the closest being only 3 mm away (Table 1). In one patient, the posterior mesh arms were placed not through the sacrospinous ligaments, but beneath the ligament, through the iliococcygeal muscle (Patient C, Fig. 4, panels a and b, Supplemental Video). There were no suspicious findings in either the three-month or one-year follow-up clinical examinations (Supplemental Table 1), but in this patient, the posterior mesh arm was closest to the pudendal neurovascular bundle (4 mm away, on average) (Table 1; Supplemental Table 1).

In the midsagittal T1 images of patients A, C, D, E, and F, the distal part of the mesh extended below (caudal to) the bladder neck and lay parallel to the urethra. The portion of the urethra having mesh underneath it ranged from 19% to 55% of the total urethra length (Table 1; Fig. 4, panels c and d). No voiding dysfunction was observed.

Discussion

In this study, we developed techniques to measure the implanted mesh dimensions and location relative to important pelvic anatomical structures based on 3D reconstruction of postoperative MR-images after anterior compartment prolapse surgery using MR-visible Fe_3O_4-polypropylene meshes. This allowed us to compare the dimensions and location of the actual implanted mesh to the manufacturer's recommendations. Preliminary findings revealed that implanted meshes are >40% shorter than the designed mesh length. We demonstrated that the measurements of the mesh location related to the ischial spines and neurovascular bundles are feasible in different subjects and stable within the same patient over time. We also correlated these measurements with the clinical findings. The data allowed us to evaluate mesh placement deviations from manufacturer recommendations[12,13] and to quantify the safety margin achieved in order to avoid structures with high risk of injury or complications.

The ability to visualize iron-loaded mesh grafts and their 3D reconstruction has been recently published.[11,14,20-22] This study extends the field by introducing objective measurement techniques that could be used clinically when evaluating mesh implantation techniques, in surgery training programs, and in situations of recurrent POP or postoperative symptoms. We are not advocating that all women have preoperative and postoperative MRIs, but the mesh MR-visibility allows us to quantify and understand its placement in a

research setting or as a diagnostic tool when complications arise. We recognize that ultrasound as the imaging tool of choice in most clinical situations is very effective in visualizing mesh material between the anterior vaginal wall and the bladder, helping diagnose mesh folding or dislodgement, and in recurrent prolapse situations.[10,11,23,24] But when trying to evaluate the mesh arms passing through the deep pelvic structures and body wall, this MR-visible mesh-based technique illuminates areas of the postoperative pelvic "situs" that were hidden until now. By simultaneously capturing the entire pelvis and mesh, this technique can provide additional information in some complex circumstances, such as postoperative pelvic pain or recurrent prolapse. In our opinion, the extended time expenditure and higher costs of this technique can be justified in these special cases.

Postoperative mesh "shrinkage" is a commonly discussed topic with controversial opinions in the evaluation of mesh surgery outcomes.[4,7,25] Our results demonstrate that the overall implanted vertical mesh length was at least 40% shorter in the three-month and one-year postoperative follow-up examinations compared to the original mesh design—suggesting possible mesh contraction/folding consistent with observations from other study teams regarding the existence of mesh contraction.[4,25,26] However, our measurements of mesh size reduction in early postoperative follow-up examinations are higher than reported by Letouzey et al., with 30%, 65%, and 85% mesh contraction at three-year, six-year, and eight-year ultrasound follow-up, respsectively.[4,26] Other reasons for a shorter measured postoperative mesh length include failed tension-free mesh insertion with resulting intraoperative folding[4] and a higher local infection status of the surgical site.[27] Another possible explanation for mesh folding could be that the original design's dimension is larger than needed to fit the anatomical conditions of the patient.

Interestingly, we could also detect notable variations in terms of where mesh shortening/folding occurred. Our results demonstrate that this can occur in both the anterior and posterior parts of the mesh. This might be due to the variation of the initial mesh tension during implantation or to differences in the anatomical situation in individual patients. It is also worth mentioning that even though all six cases in this trial had varying degrees of mesh shortening, only one patient reported experiencing pelvic pain in the postoperative follow-up. In this case, mesh reduction occurred in the posterior segment, matching the pain location reported during clinical examination. This may be explained by the excessive tension after shrinkage of the main mesh body against the fixated, unmovable arms carving into the surrounding scarring soft tissue. No hematoma or any sign of infection was visible on MRI in this case to further explain her condition.

The ischial spines are proximate the pudendal nerve and are commonly used as landmarks for mesh implantation. Surgery training programs recommend that intraoperatively, the ischial spine is palpated first. Then, the palpating fingers are to be moved approximately two centimeters proximal, sliding along the sacrospinous ligament with the palpating finger, to find the ideal localization for the penetration of the posterior mesh arm through the sacrospinous ligament.[12,13] Our data showed that the recommended safe penetration points for the posterior arms relative to the ischial spines were achieved. But following the further course of the posterior arms to the point closest to the actual pudendal neurovascular bundle revealed how close they truly are, with a mean of only 7 mm (left) and 5 mm (right). In our opinion, these results reinforce the recommendation to place the posterior mesh arms at least 20 mm proximal to the ischial spine into the sacrospinous ligament, as the pudendal neurovascular bundle is closer than anticipated. Our

findings provide, for the first time, quantitative measurements of the distance between implanted mesh and the pudendal neurovascular bundle in vivo, which could produce valuable feedback for mesh designers and manufacturers.

In addition, our technique also identified the deviations from the recommendations in surgical mesh placement. In patient C, both posterior mesh arms were placed below the sacrospinous ligaments into the iliococcygeal muscle, resulting in considerably closer distances of the posterior arms to the pudendal neurovascular bundles (3-5 mm) than recommended. However, it is important to mention that the clinical results did not reveal complications in this case, so we cannot conclude that placement deviation necessarily leads to intra- or postoperative complications - although our described technique revealed the smaller safety margin achieved with such deviations.

Amongst other postoperative complications, voiding dysfunctions are frequently mentioned when evaluating vaginal mesh surgery outcomes. Our results demonstrate that the implanted mesh extends below the bladder neck, but we could not detect voiding dysfunction in the postoperative clinical examination. Our findings are consistent with ultrasound studies,[19,20] but provide more reliable and accurate measurements with better image resolution and a larger field of view.

We acknowledge that the demonstrated technique is expensive, complex, and difficult to implement into a clinical routine. In order to perform these measurements, several conditions are required, such as implantation of an MR-visible mesh, postsurgical MRI with T1-weighted 2D and 3D sequences in appropriate slice thicknesses, and image processing software for 3D reconstruction and

measurements. This study was meant to develop the technique and demonstrate possible objective measurements to extend the current knowledge. This pilot study group is small and very heterogeneous with unfortunate missing follow-up and missing data. Better protocol will be needed to improve the compliance and retention of the future trail. Larger cohorts will be needed to evaluate surgery outcomes after implantation of the Seratom® E PA and Seratom® P PA implants. The changes in implanted mesh dimension and location over time and its correlation with clinical implication can then be investigated systematically in the future. We believe that the demonstrated technique can be very valuable in certain clinical settings, such as for diagnosing complex mesh complications, and for research in this field.

Conclusions

Our results demonstrate that this MRI-based measurement technique can precisely and objectively evaluate postoperative location and dimension of Fe_3O_4-polypropylene meshes, illustrate mesh placement variations, and identify possible complications.

Acknowledgements

Research efforts were partially supported by the Eunice Kennedy Shriver National Institute of Child Health and Human Development (NICHD) grants P50 HD044406 and R21 HD079908. The NICHD played no role in the conduct of the research or the decision to publish. We want to thank Dr. Bing Xie for 3D model smoothing.

References

1. Altman D, Vayrynen T, Engh ME, et al. Anterior colporrhaphy versus transvaginal mesh for pelvic-organ prolapse. N Engl J Med 2011; 364:1826-1836.
2. Jelovsek JE, Maher C, Barber MD. Pelvic organ prolapse. Lancet 2007; 369:1027-1038.
3. Brocker KA, Alt CD, Rzepka J, et al. One-year dynamic MRI follow-up after vaginal mesh repair: evaluation of clinical, radiological, and quality-of-life results. Acta Radiol 2014; 56:1002-1008.
4. Feiner B, Maher C. Vaginal mesh contraction: definition, clinical presentation, and management. Obstet Gynecol 2010; 115:325-330.
5. Campagna G, Panico G, Morciano A, et al. Vaginal mesh repair SYSTEMS for pelvic organ prolapse: Anatomical study comparing transobturator/trangluteal versus single incision techniques. Neurourol Urodyn 2017.
6. Barski D, Otto T, Gerullis H. Systematic Review and Classification of Complications after Anterior, Posterior, Apical, and Total Vaginal Mesh Implantation for Prolapse Repair. Surg Technol Int 2014; XXIV.
7. Dietz HP, Erdmann M, Shek KL. Mesh contraction: myth or reality? Am J Obstet Gynecol 2011; 204:173 e171-174.
8. Baeßler K, Aigmueller T, Albrich S, et al. Diagnosis and treatment oft he pelvic organ prolaps. Guideline of the German Society of Gynecology and Obstetrics (S2e-Level, AWMF Registry No. 015/006, April 2016). . 2016.
9. Rodrigo N, Wong V, Shek KL, et al. The use of 3-dimensional ultrasound of the pelvic floor to predict recurrence risk after pelvic reconstructive surgery. Aust N Z J Obstet Gynaecol 2014; 54:206-211.
10. Shek KL, Dietz HP, Rane A, et al. Transobturator mesh for cystocele repair: a short- to medium-term follow-up using 3D/4D ultrasound. Ultrasound Obstet Gynecol 2008; 32:82-86.
11. Chen L, Lenz F, Alt CD, et al. MRI visible Fe3O4 polypropylene mesh: 3D reconstruction of spatial relation to bony pelvis and neurovascular structures. Int Urogynecol J 2017; 28:1131-1138.
12. Fischer A. OP-Atlas Praktische UrogynäkologieBirgitt Lucas.2007. 366 p.
13. Moore RD, Mitchell GK, Miklos JR. Single-incision vaginal approach to treat cystocele and vault prolapse with an anterior wall mesh anchored apically to the sacrospinous ligaments. Int Urogynecol J 2012; 23:85-91.
14. Brocker KA, Lippus F, Alt CD, et al. Magnetic resonance-visible polypropylene mesh for pelvic organ prolapse repair. Gynecol Obstet Invest 2014; 79:101-106.
15. Farthmann J, Watermann D, Niesel A, et al. Lower exposure rates of partially absorbable mesh compared to nonabsorbable mesh for cystocele treatment: 3-year follow-up of a prospective randomized trial. Int Urogynecol J 2012; 24:749-758.
16. Betschart C, Chen L, Ashton-Miller JA, et al. On pelvic reference lines and the MR evaluation of genital prolapse: a proposal for standardization using the Pelvic Inclination Correction System. Int Urogynecol J 2013; 24:1421-1428.
17. Brandon CJ, Lewicky-Gaupp C, Larson KA, et al. Anatomy of the perineal membrane as seen in magnetic resonance images of nulliparous women. Am J Obstet Gynecol 2009; 200:583 e581-586.

18. Fritz J, Dellon AL, Williams EH, et al. 3-Tesla High-Field Magnetic Resonance Neurography for Guiding Nerve Blocks and Its Role in Pain Management. Magn Reson Imaging Clin N Am 2015; 23:533-545.
19. Ansquer Y, Fernander P, Aimot S, et al. MRI urethrovesical junction mobility is associated with global pelvic floor laxity in female stress incontinence. Acta Obstet Gynecol Scand 2007; 86:1243-1250.
20. Sindhwani N, Feola A, De Keyzer F, et al. Three-dimensional analysis of implanted magnetic-resonance-visible meshes. Int Urogynecol J 2015; 26:1459-1465.
21. Ciritsis A, Hansen NL, Barabasch A, et al. Time-Dependent Changes of Magnetic Resonance Imaging-Visible Mesh Implants in Patients. Invest Radiol 2014; 49:439-444.
22. Ciritsis A, Truhn D, Hansen NL, et al. Positive Contrast MRI Techniques for Visualization of Iron-Loaded Hernia Mesh Implants in Patients. PLoS One 2016; 11:e0155717.
23. Shek KL, Dietz HP. Imaging of slings and meshes. Australas J Ultrasound Med 2014; 17:61-71.
24. Dietz HP. Pelvic Floor Ultrasound: A Review. Clin Obstet Gynecol 2017; 60:58-81.
25. Svabik K, Martan A, Masata J, et al. Ultrasound appearances after mesh implantation--evidence of mesh contraction or folding? Int Urogynecol J 2011; 22:529-533.
26. Letouzey V, Deffieux X, Levaillant J, et al. Ultrasound evaluation of polypropylene mesh contraction at long term after vaginal surgery for cystocele repair. 34th Annual Scientific Meeting of the International Urogynecological Association, June 2009. Lake Como, Italy.
27. Mamy L, Letouzey V, Lavigne JP, et al. Correlation between shrinkage and infection of implanted synthetic meshes using an animal model of mesh infection. Int Urogynecol J 2010; 22:47-52.

Figure Legend

Figure 1

Example of a 3D model reconstruction of the implanted Fe_3O_4-polypropylene mesh within the same patient (A) at both examination points. The mesh was marked with yellow dots at the 3-month examination (Panels a, b, c, g) and with green dots at the 1-year

examination (Panels d, e, f, g) on T1-weighted MR-images. The 3D models show the location of the mesh and its fixational arms according to the bony pelvic frame and the sacrospinous ligament (marked in blue at panels c, f, and g).

Figure 2

Example of postoperative mesh changes in two patients. The mesh designed dimension is shown as an insert in the upper middle of the figure. Mesh shrinkage or possible double layering can be observed in the distal (anterior) mesh part (patient A at 3-month follow-up, panels a-c) or proximal (posterior) mesh part (patient E at 1-year follow-up, panels d-f). In the postoperative follow-up, the total vertical mesh length (red line, panels a and d) appeared smaller (patient A: 55 mm; patient E: 60 mm) than the presurgical size (103 mm). Panels b, c, e, and f demonstrate the cranialcaudal view onto the mesh body (Seratom E PA®, yellow dots/area). The sacrospinous ligaments are marked blue. Ant: anterior; L: left; Pos: posterior; R: right.

Figure 3

Close-up image of mesh (region of interest marked as a white block in the orientation insert) in relation to neurovascular structures and bony pelvis describing possible measurements that can be performed with this technique, e.g. the shortest distance between alloplastic material and anatomic structure of interest. Panel a demonstrates in a craniocaudal view the distance (arrow-headed line, 13 mm) measured in 3D space between the left posterior arm and the left pudendal neurovascular bundle (red dots). Panel b demonstrates the distance (arrow-headed line, 22 mm) between the left middle arm and the obturator neurovascular bundle (orange

dots). Panel c describes the distance (arrow-headed line, 27 mm) from the penetration point of the posterior right arm through the sacrospinous ligament to the right ischial spine (IS_R).

Figure 4

With this visualization technique, variations in postoperative mesh location can be revealed as demonstrated here in the 3D pelvic model of patient C. Panels a and b show the posterior mesh arm's spatial relationship to the sacrospinous ligaments (dark blue). Both panel a (caudocranial view) and panel b (view from left caudal, outside to inside) reveal the gap between both posterior mesh arms and the sacrospinous ligaments (Supplemental Video). Panel c shows the 3D model of the mesh (yellow dots) and bladder (light blue) with the middle sagittal MR-image. The distal part of the mesh runs parallel to the urethra (arrow). Panel d displays this middle sagittal T2 image. The urethral length (light blue line) and the amount of urethra covered by the distal part of the mesh body (pink arrow) were measured (Panel d). The clinical follow-up examinations showed no voiding disorders. Red dot points out the left ischial spine; PS: pubic symphysis; R: rectum; SB: small bowel.

Supplemental Figure 1

Partially absorbable anterior vaginal six-arm meshes applied in this trial (Seratom E PA®, Seratom P PA®) with important mesh dimensions.

A: Vertical mesh length; B: Total mesh width; C1: Distance between anterior and middle arm; C2: Distance between middle and posterior arm; D: Width, anterior and posterior arm

; E: Width, middle arm; F: Anterior-middle arm length (C1)/whole mesh length (A), ratio.

Supplemental Video

The supplemental video shows the 3D pelvic models of patient C from caudocranial view (Figure 4, panel a) rotating to the view in figure 4, panel b. The video reveal the gap between both posterior mesh arms and the sacrospinous ligaments demonstrating deviation of posterior mesh arm placement from the recommendation.

Table 1. Measurements performed after 3D-reconstruction of the MR-visible mesh in the six study patients

Measurement Parameters	Seratom E PA®	Seratom P PA®	MRI-Based M			
			3-month postoperative MRI			
			A (E)	B (P)	C (E)*^{Trim}	D (P)
Implanted Mesh Size	**Original Measurement**					
Total vertical mesh length	103 (83^{*trim})	90 (70^{*trim})	55	54	45	53
Anterior segment length	57	42	10	10	NA	35
Posterior segment length	46	48	45	44	NA	18
Anterior/Posterior segment ratio	1.24	0.875	0.22	0.23	NA	1.94
Distances of mesh arms to nerve bundles	**Recommended Distance**					
Left posterior arm to left pudendal bundle	>20	>20	9	6	3	11
Right posterior arm to right pudendal bundle	>20	>20	14	3	5	5
Left anterior arm to left obturator bundle	>15	>15	21	16	14	19
Right anterior arm to right obturator bundle	>15	>15	15	17	11	33
Posterior mesh arm insertion	**Recommended Distance**					
Left posterior arm to ischial spine	>20	>20	15	13	19	33
Right posterior arm to ischial spine	>20	>20	27	9	13	33
Relation to urethra						
Urethra length	NA	NA	31	NA	24	32
Mesh beneath UVJ	0	0	17	NA	12	10
Proportion of urethral length covered by mesh, %	0	0	55	NA	50	31

Measurements are in mm

A, B, C, D, E, F: Patient ID; (E): patient with Seratom E PA MR®; (P) patient with Seratom P PA MR®; MRI: magnetic resonance imaging; NA: not applicable; UVJ: ureterovesical junction; *^{Trim}: Mesh trimmed including anterior arms by surgeon during surgery; mesh-length therefore shortened approximately 20 mm; segment mesh measurements not applicable (NA); Grey cells demonstrate patients with mesh location not meeting the mesh implantation recommendation.

Table 1. Measurements performed after 3D-reconstruction of the MR-visible mesh in the six study patients

Measurement Parameters	Seratom E PA®	Seratom P PA®	MRI-Based M			
			3-month postoperative MRI			
			A (E)	B (P)	C (E)*^{Trim}	D (P)
Implanted Mesh Size	**Original Measurement**					
Total vertical mesh length	103 (83^{*trim})	90 (70^{*trim})	55	54	45	53
Anterior segment length	57	42	10	10	NA	35
Posterior segment length	46	48	45	44	NA	18
Anterior/Posterior segment ratio	1.24	0.875	0.22	0.23	NA	1.94
Distances of mesh arms to nerve bundles	**Recommended Distance**					
Left posterior arm to left pudendal bundle	>20	>20	9	6	3	11
Right posterior arm to right pudendal bundle	>20	>20	14	3	5	5
Left anterior arm to left obturator bundle	>15	>15	21	16	14	19
Right anterior arm to right obturator bundle	>15	>15	15	17	11	33
Posterior mesh arm insertion	**Recommended Distance**					
Left posterior arm to ischial spine	>20	>20	15	13	19	33
Right posterior arm to ischial spine	>20	>20	27	9	13	33
Relation to urethra						
Urethra length	NA	NA	31	NA	24	32
Mesh beneath UVJ	0	0	17	NA	12	10
Proportion of urethral length covered by mesh, %	0	0	55	NA	50	31

MA, B, C, D, E, F: Patient ID; (E): patient with Seratom E PA MR®; (P) patient with Seratom P PA MR®; MRI: magnetic resonance imaging; NA: not applicable; UVJ: ureterovesical junction; *^{Trim}: Mesh trimmed including anterior arms by surgeon during surgery; mesh-length therefore shortened approximately 20 mm; segment mesh measurements not applicable (NA); Grey cells demonstrate patients with mesh location not meeting the mesh implantation recommendation.
easurements are in mm

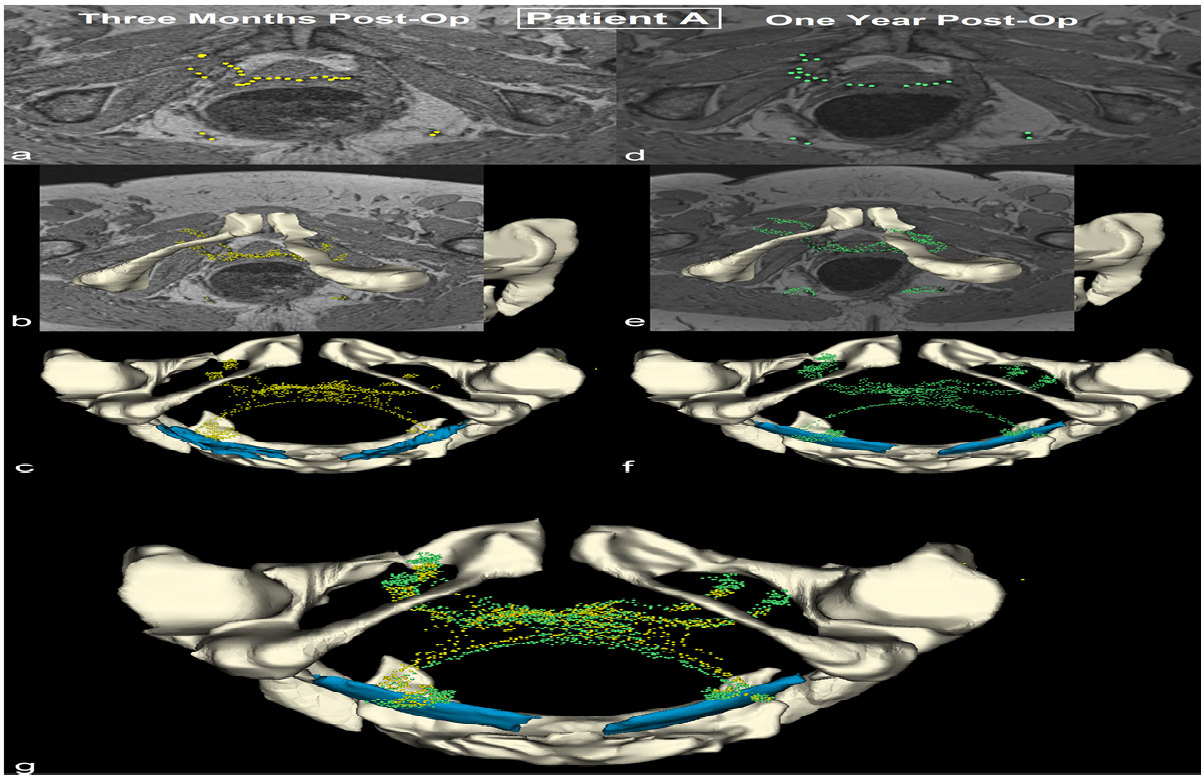

Figure 1 .

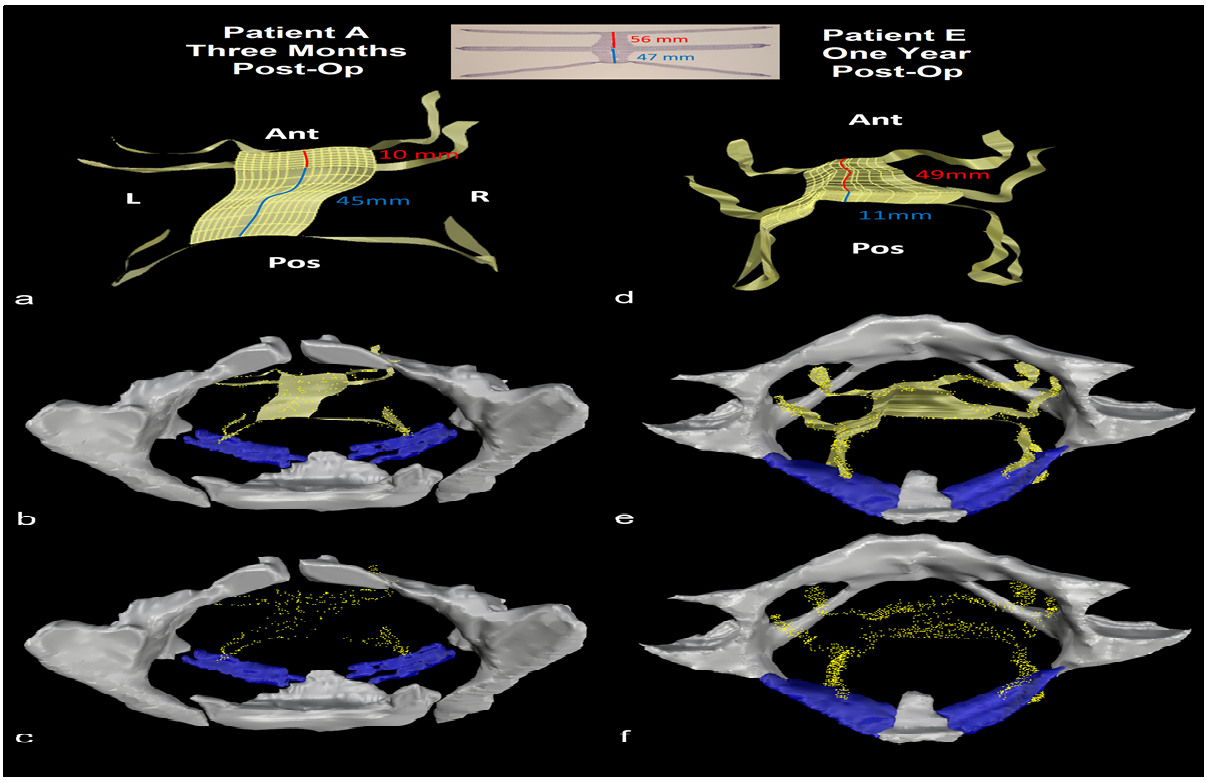

Figure 2 .

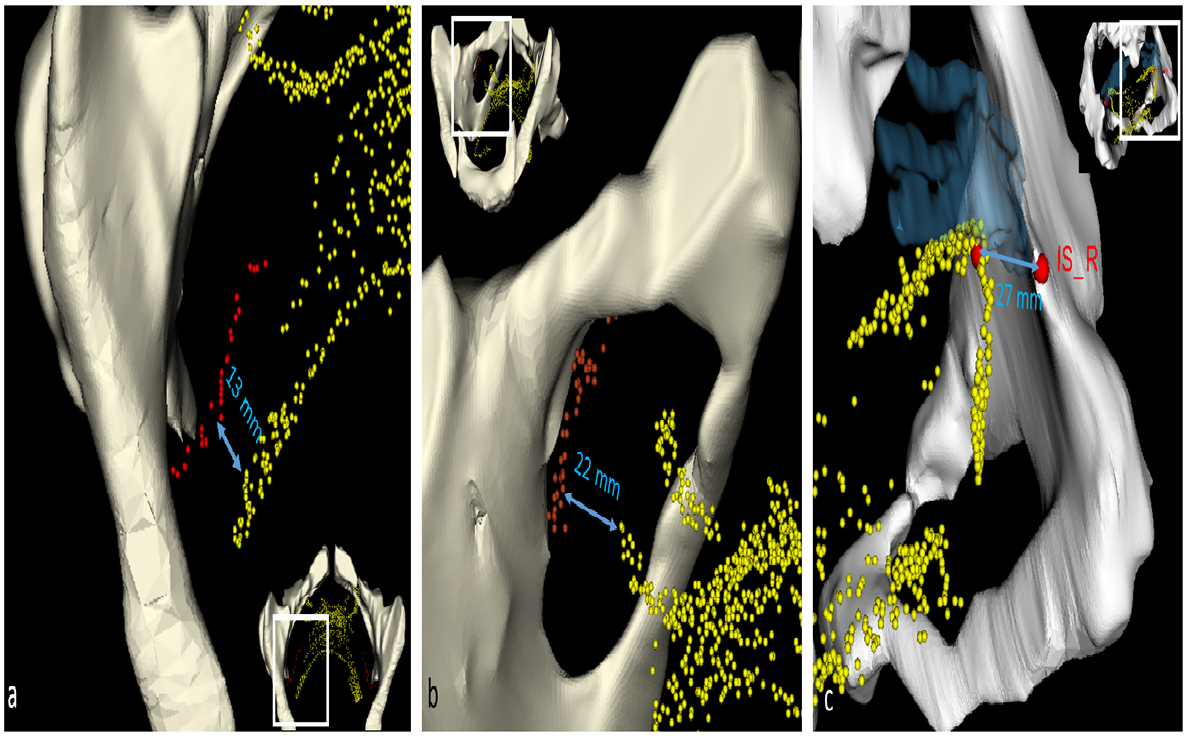

Figure 3 .

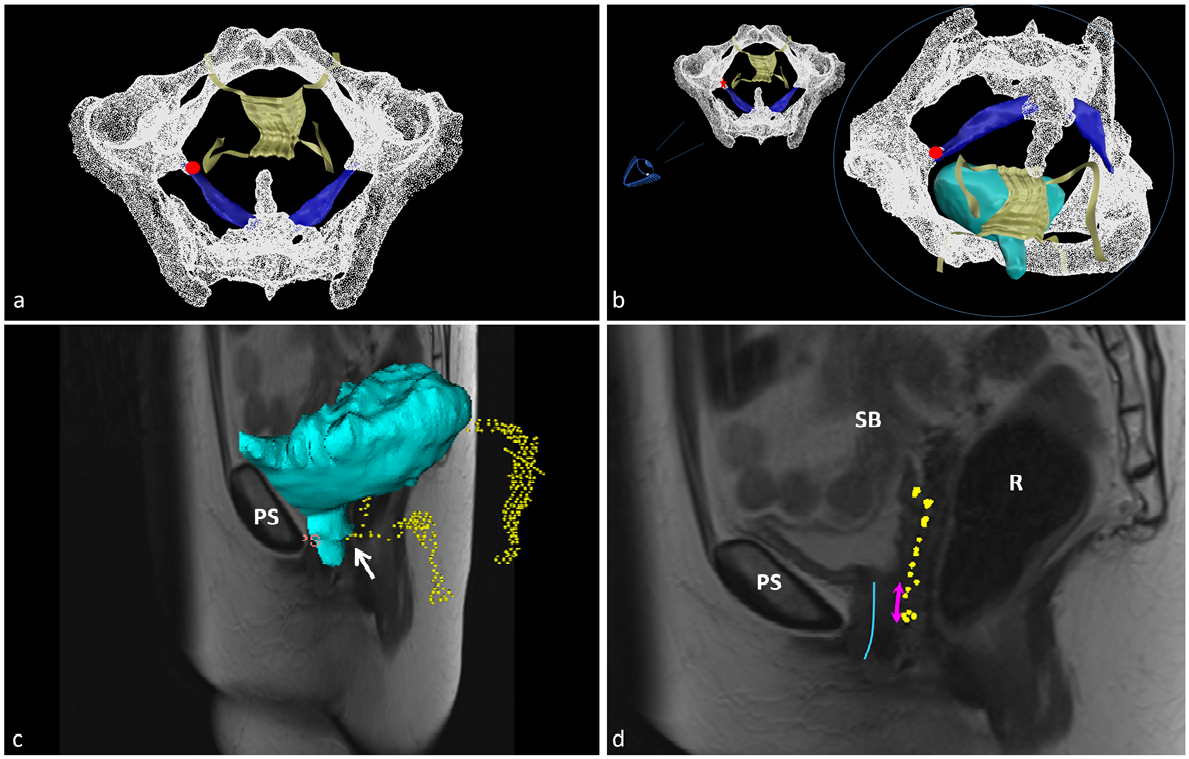

Figure 4 .

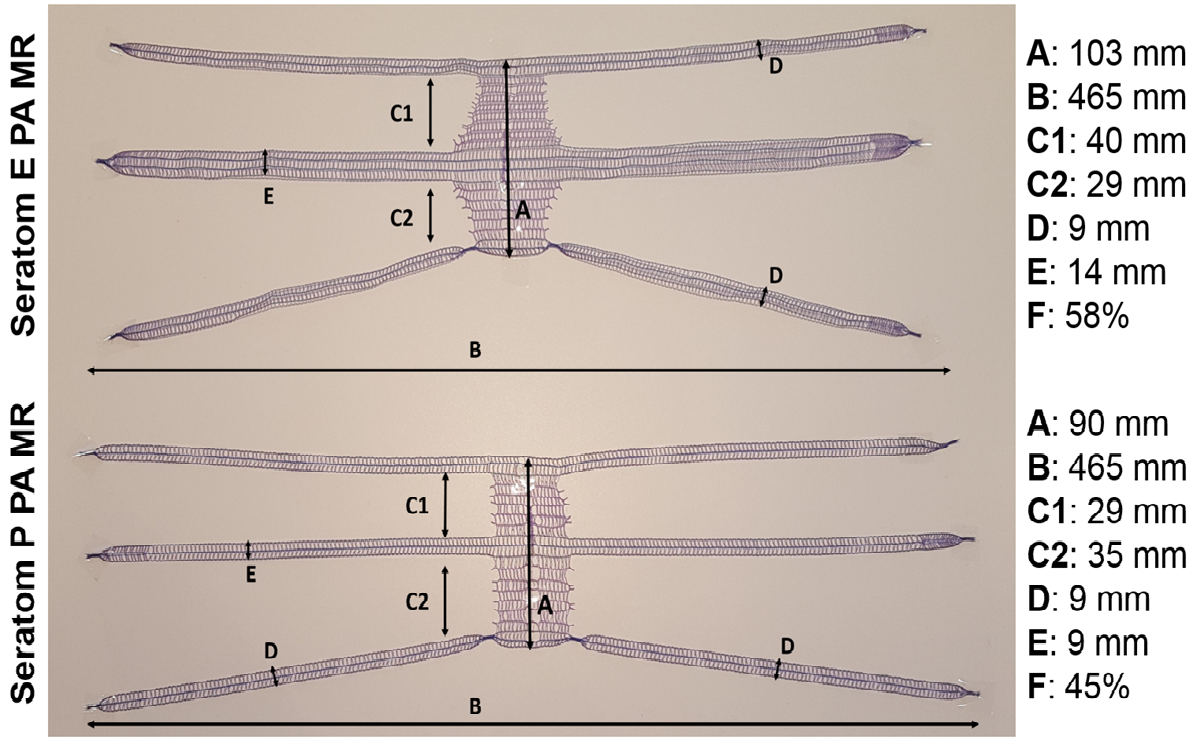

Supplemental Figure 1 .